Proceedings of the 3rd International Conference on
Fracture Fatigue and Wear, pp. 127-133, 2014

# VIBRATION ANALYSIS OF CRACKED PLATE USING HIGHER-ORDER SHEAR DEFORMATION THEORY

Loc V. Tran[1], P. Phung-Van[1,3], Vinh Phu Nguyen[2], M. Abdel Wahab[3] and H. Nguyen-Xuan [1]

[1] Division of Computational Mechanics, Ton Duc Thang University Ho Chi Minh City, Vietnam
[2]Cardiff University, Queen's Buildings, The Parade, Cardiff CF24 3AA, Wales, UK
[3]Department of Mechanical Construction and Production, Faculty of Engineering and Architecture, Ghent University, Belgium

**Abstract:** A novel and effective formulation that combines the eXtended IsoGeometric Approach (XIGA) and Higher-order Shear Deformation Theory (HSDT) is proposed to study the free vibration of cracked plates. XIGA utilizes the Non-Uniform Rational B-Spline (NURBS) functions with their inherent arbitrary high order smoothness, which permit the $C^1$ requirement of the HSDT model. Two numerical examples are provided to show excellent performance of the proposed method compared with other published solutions in the literature.

**Keywords:** cracked plate; non-uniform rational b-spline; isogeometric analysis; higher-order shear deformation theory

## 1 INTRODUCTION

Plate structures play an increasing important role in engineering applications. They thus were researched since long time from static to dynamic and buckling analysis [1-5]. From the literature, these works are carried out for designing the plate structures without the presences of cracks or flaws. It is known that in service, the cracks are generated and grown when subjected to large cyclic loading. They lead to a reduction of the load carrying capacity of the structures. To clearly understand the dynamic behaviour of plate with initial cracks is hence too necessary. This problem has been interesting by many scientists with various methods: Stahl and Keer [6] and Liew et al. [7] with analytical solutions, Finite Element Method (FEM) [9], eXtended Finite Element Method (XFEM) [8,10], etc. Among them, XFEM is known as a robust numerical method, which uses enrichment functions to model discontinuities independent of the finite element mesh. Recently, Natarajan et al. [11] extended this method for dynamic analysis of FGM plate based on the FSDT model. This model is simple to implement and is applicable to both thick and thin FGM plates. However, the accuracy of solutions will be strongly dependent on the Shear Correction Factors (SCF) of which their values are quite dispersed through each problem.

In this paper, we develop the Higher-order Shear Deformation Theory (HSDT) model that includes higher-order terms in the approximation of the displacement field for modelling the plates. It is worth mentioning that this model requires $C^1$-continuity of the generalized displacements leading to the second-order derivative of the stiffness formulation which causes some obstacles in standard $C^0$ finite formulations. Fortunately, it is shown that such a $C^1$-HSDT formulation can be easily achieved using a NURBS-based isogeometric approach [12]. In addition, to capture the discontinuous phenomenon in the cracked plates, the enrichment functions is incorporated with NURBS basic functions to create a novel method as so-called eXtended Isogeometric Analysis (XIGA) [13]. Herein, our study focuses on investigating the vibration of the cracked plates with an initial crack. Two numerical examples are given to show the performance of the proposed method and results obtained are compared to other published methods in the literature.

## 2 GOVERNING EQUATIONS FOR PLATES

To consider the effect of shear deformation directly, the five-parameter displacement field based on higher-order shear deformation theory is defined as

$$\begin{aligned} u(x,y,z) &= u_0 - zw_{,x} + \left(z - \tfrac{4}{3h^2}z^3\right)\beta_x \\ v(x,y,z) &= v_0 - zw_{,y} + \left(z - \tfrac{4}{3h^2}z^3\right)\beta_y \quad , \quad \left(\frac{-h}{2} \le z \le \frac{h}{2}\right) \\ w(x,y) &= w_0 \end{aligned} \tag{1}$$

where $u_0, v_0, w$ are the axial displacements and $\beta_x, \beta_y$ are the rotations in the *x* and *y* axes, respectively.

The strains of the mid-surface deformation are given by

$$\begin{Bmatrix} \boldsymbol{\varepsilon} \\ \boldsymbol{\gamma} \end{Bmatrix} = \begin{Bmatrix} \boldsymbol{\varepsilon}_0 + z\boldsymbol{\kappa}_1 + \left(z - \tfrac{4}{3h^2}z^3\right)\boldsymbol{\kappa}_2 \\ \left(1 - \tfrac{4}{h^2}z^2\right)\boldsymbol{\beta} \end{Bmatrix} \tag{2}$$

Using the Hamilton principle, the weak form for free vibration analysis of a plate can be expressed as:

$$\int_\Omega \delta\boldsymbol{\varepsilon}^T \mathbf{D}^b \boldsymbol{\varepsilon} \mathrm{d}\Omega + \int_\Omega \delta\boldsymbol{\gamma}^T \mathbf{D}^s \boldsymbol{\gamma} \mathrm{d}\Omega = \int_\Omega \delta\tilde{\mathbf{u}}^T \mathbf{m} \ddot{\tilde{\mathbf{u}}} \mathrm{d}\Omega \tag{3}$$

where $\mathbf{D}^b$ and $\mathbf{D}^s$ are the material matrices

Herein, the mass matrix **m** is calculated according to consistent form as follow

$$\mathbf{m} = \begin{bmatrix} I_1 & I_2 & I_4 \\ I_2 & I_3 & I_5 \\ I_4 & I_5 & I_6 \end{bmatrix} \text{ with } I_i = \int_{-h/2}^{h/2} \rho_e \left(1, z, z^2, \left(z - \tfrac{4}{3h^2}z^3\right), z\left(z - \tfrac{4}{3h^2}z^3\right), \left(z - \tfrac{4}{3h^2}z^3\right)^2\right) \mathrm{d}z \tag{4}$$

and

$$\tilde{\mathbf{u}} = \begin{Bmatrix} \mathbf{u}_1 \\ \mathbf{u}_2 \\ \mathbf{u}_3 \end{Bmatrix}, \quad \mathbf{u}_1 = \begin{Bmatrix} u_0 \\ v_0 \\ w \end{Bmatrix}; \mathbf{u}_2 = -\begin{Bmatrix} w_{,x} \\ w_{,y} \\ 0 \end{Bmatrix}; \mathbf{u}_3 = \begin{Bmatrix} \beta_x \\ \beta_y \\ 0 \end{Bmatrix} \tag{5}$$

## 3 AN EXTENDED ISOGEOMETRIC CRACKED PLATE FORMULATION

# 3.1 A brief of B-spline/NURBS functions

A knot vector $\Xi = \{\xi_1, \xi_2, ..., \xi_{n+p+1}\}$ is defined as a sequence of knot value $\xi_i \in R$, $i = 1, ...n+p$. If the first and the last knots are repeated *p*+1 times, the knot vector is called an open knot. Through open knot, the B-spline basis functions $N_{i,p}(\xi)$ are defined by the following recursion formula

$$\begin{aligned} N_{i,p}(\xi) &= \frac{\xi - \xi_i}{\xi_{i+p} - \xi_i} N_{i,p-1}(\xi) + \frac{\xi_{i+p+1} - \xi}{\xi_{i+p+1} - \xi_{i+1}} N_{i+1,p-1}(\xi) \\ \text{as } p = 0,\ N_{i,0}(\xi) &= \begin{cases} 1 & if \quad \xi_i < \xi < \xi_{i+1} \\ 0 & \text{otherwise} \end{cases} \end{aligned} \tag{6}$$

To present exactly some curved geometries (e.g. circles, cylinders, spheres, etc.) the Non-Uniform Rational B-Splines (NURBS) functions are used. Be different from B-spline, each control point of NURBS has additional value called an individual weight $w_i$ [12]. Then the NURBS functions can be expressed as

$$R_i(\xi,\eta) = \frac{N_i w_i}{\sum N_i(\xi,\eta) w_i} \tag{7}$$

## 3.2 Cracked plate formulation eXtended IsoGeometric Analysis (XIGA)

To capture the local discontinuous and singular fields, the new enriched functions are added according to idea of XFEM as follow:

$$\mathbf{u}^h(\mathbf{x}) = \sum_{I\in S} R_I(\boldsymbol{\xi})\mathbf{q}_I^{std} + \sum_{J\in S^{enr}} R_J^{enr}(\boldsymbol{\xi})\mathbf{q}_J^{enr} \tag{8}$$

Here, the NURBS basis functions are utilized instead of the Lagrange polynomials to create a new numerical procedure – so-called eXtended IsoGeometric Analysis (XIGA) [13,14]. $R_J^{enr}$ are the enrichment functions associated with node *J* located in enriched domain $S^{enr}$ which is splitted up two parts including: a set $S^c$ for Heaviside enriched control points and a set $S^f$ for crack tip enriched control points as shown in Fig. 1.

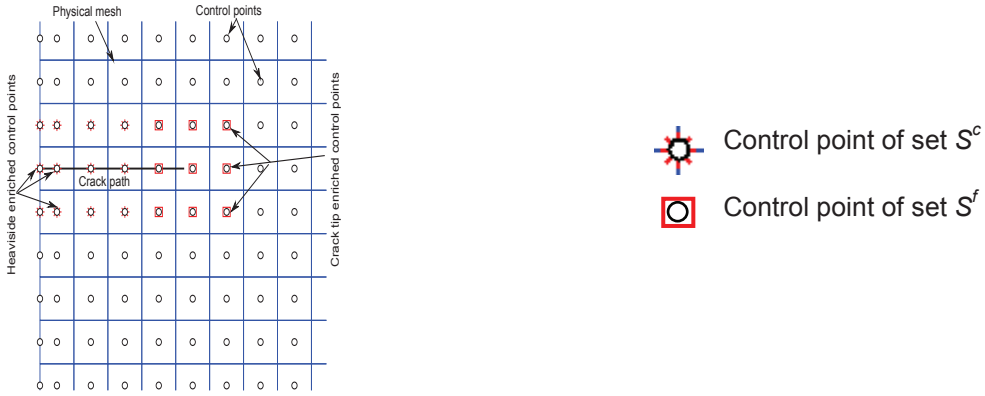


**Fig. 1** Illustration of the nodal sets $S^c$, $S^f$ for a quadratic NURBS mesh

To describe the discontinuous displacement field, the enrichment function is given by

$$R_J^{enr}(\boldsymbol{\xi}) = R_J(\boldsymbol{\xi})\left(H(\mathbf{x}) - H(\mathbf{x}_J)\right), \quad J \in S^c \tag{9}$$

where $H(\mathbf{x})$ is the Heaviside function and the singularity field near crack tip is modified by the branching functions (see more details in Ref [10]) as follow

$$R_J^{enr}(\boldsymbol{\xi}) = R_J(\boldsymbol{\xi})\left(\sum_{L=1}^{4}\left(G_L(r,\theta) - G_L(r_J,\theta_J)\right)\right), \quad J \in S^f \tag{10}$$

where

$$G_L(r,\theta) = \begin{cases} r^{3/2}\left[\sin\dfrac{\theta}{2} \quad \cos\dfrac{\theta}{2} \quad \sin\dfrac{3\theta}{2} \quad \cos\dfrac{3\theta}{2}\right] & \text{for } u_0,\ v_0,\ w \text{ variables} \\ r^{1/2}\left[\sin\dfrac{\theta}{2} \quad \cos\dfrac{\theta}{2} \quad \sin\dfrac{\theta}{2}\sin\theta \quad \cos\dfrac{\theta}{2}\cos\theta\right] & \text{for } \beta_x,\ \beta_x \text{ variables} \end{cases} \tag{11}$$

in which *r* and $\theta$ are polar coordinates in the local crack tip coordinate system.

## 3.3 Cracked plate formulation based on HSDT

Now, using the displacement field approximated in Eq. (8), the strain matrices including in-plane and shear strains can be rewritten as:

$$\left[\boldsymbol{\varepsilon}_0^T \ \boldsymbol{\kappa}_1^T \ \boldsymbol{\kappa}_2^T \ \boldsymbol{\varepsilon}_s^T\right]^T = \sum_{I=1}^{m\times n}\left[\left(\mathbf{B}_I^m\right)^T \ \left(\mathbf{B}_I^{b1}\right)^T \ \left(\mathbf{B}_I^{b2}\right)^T \ \left(\mathbf{B}_I^s\right)^T\right]^T \mathbf{q}_I \tag{12}$$

in which the unknown vector **q** contains both displacements and enriched DOFs, and

$$\mathbf{B} = \left[\mathbf{B}^{std} \middle| \mathbf{B}^{enr}\right] \tag{13}$$

where $\mathbf{B}^{std}$ and $\mathbf{B}^{enr}$ are the standard and enriched strain matrices of $\mathbf{B}$.

Substituting Eq. (2) with relation in Eq. (12) into Eq. (3), the formulations of free vibration problem can be rewritten as follow:

$$\left(\mathbf{K}-\omega^2\mathbf{M}\right)\mathbf{d}=\mathbf{0} \tag{14}$$

where $\omega \in \mathrm{R}^+$ are the natural frequency and the global stiffness matrix **K** is given by:

$$\mathbf{K}=\int_\Omega \left\{\mathbf{B}^m \quad \mathbf{B}^{b1} \quad \mathbf{B}^{b2}\right\}\mathbf{D}^b\left\{\mathbf{B}^m \quad \mathbf{B}^{b1} \quad \mathbf{B}^{b2}\right\}^T+\mathbf{B}^{sT}\mathbf{D}^s\mathbf{B}^s \mathrm{d}\Omega \tag{15}$$

## 4 NUMERICAL RESULTS

First, let study the natural frequencies of a thin isotropic cracked plate (ν=0.3) with dimension $L\times W\times h$ has an initial crack at center as shown in Fig. 2a.

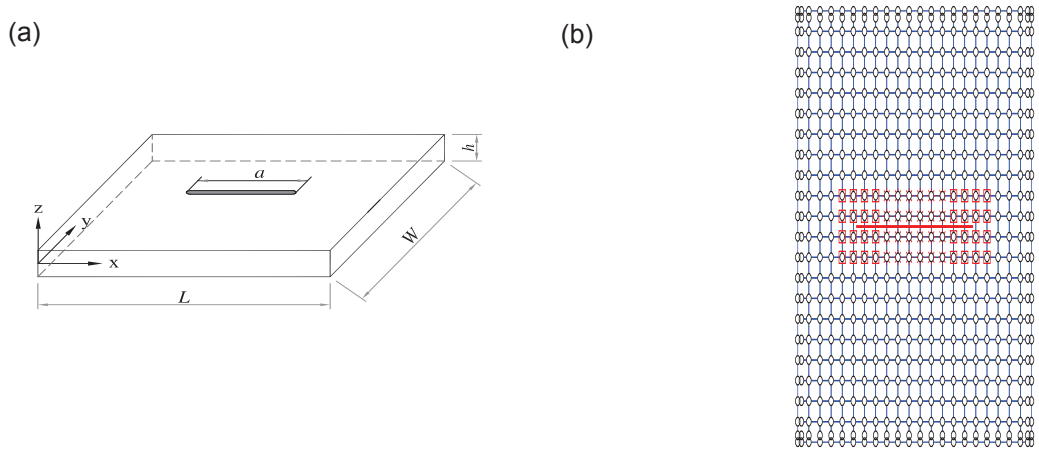


**Fig. 2** The plate with a center crack: (a) model; (b) mesh of 21x21 cubic NURBS elements

The relation between non-dimension frequencies $\hat{\omega}=\omega L^2\sqrt{\rho h/D}$ and crack length ratio according to mesh 21x21 as shown in Fig2b is reported in Table1. The obtained results from XIGA are in good agreement compared to both analytical solution [6,7] and XFEM [8] using 20x20 nine-node Lagrange elements. For clearer vision, the comparison of first five frequencies between the present result and that of Stahl [6] and Liew [7] is depicted in Fig.3. It is revealed that the frequencies decrease via increase in crack length ratio. For example, the values of frequency according to change of mode from 1 to 5 drop up to 18.3%, 67.3%, 5.3%, 40.8% and 23.7% of its initial values corresponding to an intact plate, respectively. It is concluded that the magnitude of the frequency according to anti-symmetric modes through the y-axis, which is perpendicular with cracked path (e.g. mode 2, mode 4, shown in Fig. 4), is much more affected by the crack length. Here, the discontinuous displacement is shown clearly along crack path.

**Table 1** Non dimensional natural frequency of an isotropic square plate with central crack *L/h*=1000

| Mode Number | Source | Crack length ratio *a/L* | | | | | | |
|---|---|---|---|---|---|---|---|---|
| | | 0 | 0.2 | 0.4 | 0.5 | 0.6 | 0.8 | 1 |
| 1 | Stahl [6] | 19.7390 | 19.3050 | 18.2790 | 17.7060 | 17.1930 | 16.4030 | 16.1270 |
| | Liew [7] | 19.7400 | 19.3800 | 18.4400 | 17.8500 | 17.3300 | 16.4700 | 16.1300 |
| | XFEM [8] | 19.7390 | 19.3050 | 18.2780 | 17.7070 | 17.1800 | 16.4060 | 16.1330 |
| | XIGA | 19.7392 | 19.3846 | 18.4617 | 17.8989 | 17.3576 | 16.5157 | 16.1345 |
| 2 | Stahl [6] | 49.3480 | 49.1700 | 46.6240 | 43.0310 | 37.9780 | 27.7730 | 16.1270 |
| | Liew [7] | 49.3500 | 49.1600 | 46.4400 | 42.8200 | 37.7500 | 27.4300 | 16.1300 |
| | XFEM [8] | 49.3480 | 49.1810 | 46.6350 | 43.0420 | 37.9870 | 27.7530 | 17.8260 |
| | XIGA | 49.3501 | 49.1906 | 47.1197 | 44.7124 | 39.3469 | 29.1186 | 16.1345 |
| 3 | Stahl [6] | 49.3480 | 49.3280 | 49.0320 | 48.6970 | 48.2230 | 47.2560 | 46.7420 |
| | Liew [7] | 49.3500 | 49.3100 | 49.0400 | 48.7200 | 48.2600 | 47.2700 | 46.7400 |
| | XFEM [8] | 49.3480 | 49.3240 | 49.0320 | 48.6850 | 48.2140 | 47.2010 | 46.7340 |
| | XIGA | 49.3501 | 49.3292 | 49.0903 | 48.6328 | 48.3547 | 47.3448 | 46.7376 |
| 4 | Stahl [6] | 78.9570 | 78.9570 | 78.6020 | 77.7330 | 75.5810 | 65.7320 | 46.7420 |
| | Liew [7] | 78.9600 | 78.8100 | 78.3900 | 77.4400 | 75.2300 | 65.1900 | 46.7400 |
| | XFEM [8] | 78.9550 | 78.9450 | 78.6000 | 77.7100 | 75.5790 | 65.7150 | 49.0990 |
| | XIGA | 78.9589 | 78.9452 | 78.6507 | 77.6642 | 76.0779 | 67.2308 | 46.7376 |
| 5 | Stahl [6] | 98.6960 | 93.9590 | 85.5100 | 82.1550 | 79.5880 | 76.3710 | 75.2850 |
| | Liew [7] | 98.7000 | 94.6900 | 86.7100 | 83.0100 | 80.3200 | 76.6000 | 75.2800 |
| | XFEM [8] | 98.6980 | 93.8930 | 85.4500 | 82.1080 | 79.5560 | 76.3510 | 75.2750 |
| | XIGA | 98.7292 | 94.5834 | 86.6987 | 82.7347 | 80.3835 | 76.7866 | 75.2823 |

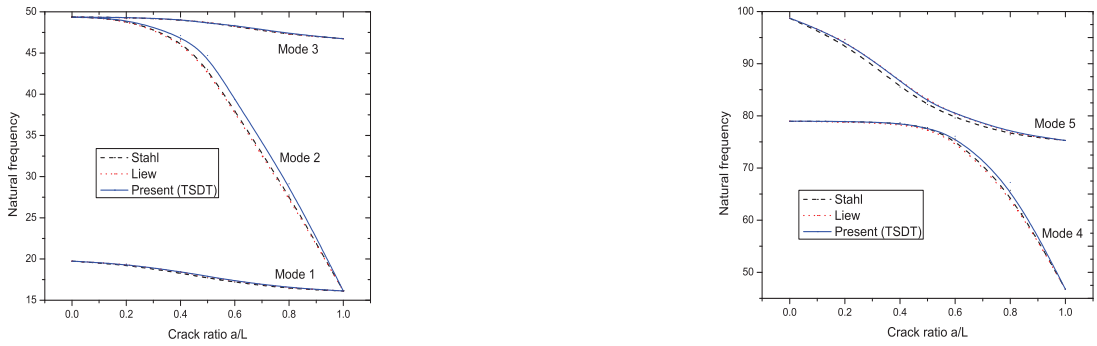


**Fig. 3** Variation of first five mode frequencies via length crack ratio

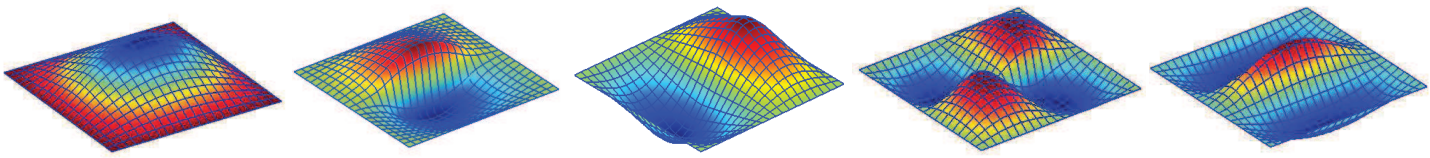


**Fig. 4** The first five mode shapes of simply supported plate having center crack with *a/L* =0.8

Next, an annular plate with uniform thickness *h*, outer radius *R* and inner one *r* as shown in Fig. is studied. The plate is made of Al/$Al_2O_3$ FGM with properties : $E_c$=70 GPa , $E_m$=380 GPa , $\nu_c=\nu_m$=0.3, $\rho_c$=2707 kg/$m^3$, $\rho_m$=3800 kg/$m^3$. The FGM is homogenized according to the Mori-Tanaka scheme with the effective values of Young's modulus *E* and Poisson's ratio $\nu$ are calculated from the effective bulk and shear modulus [4] as below :

$$E_e = \frac{9K_e\mu_e}{3K_e+\mu_e}, \qquad \nu_e = \frac{3K_e-2\mu_e}{2(3K_e+\mu_e)} \tag{16}$$

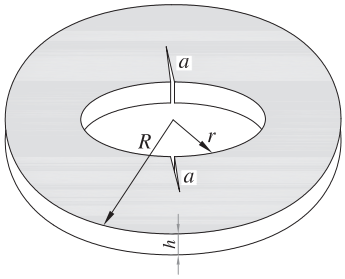


**Fig. 5** The model of annular plate.

Table 2 tabulates the frequency parameter of the annular Al/$Al_2O_3$ plates via outer radius to inner radius ratio *R/r* and radius to thickness ratio *R/h* according to *n*=1. It is concluded that the frequency parameters decrease sequentially following to increase in inner radius to outer radius ratio *r/R.* To enclose this section the first four mode shapes of annular FGM plate are depicted in Fig. 6.

**Table 2** The frequency parameter $\tilde{\omega} = \omega(R-r)^2 / h\sqrt{\rho_c / E_c}$ of an annular pate via inner radius to outer radius ratio *r/R* and radius to thickness ratio *R/h* according to *n*=1.

| *R/h* | *r/R* | Mode number | | | | |
|---|---|---|---|---|---|---|
| | | 1 | 2 | 3 | 4 | 5 |
| 2 | 0 | 1.2786 | 1.7682 | 2.3336 | 2.7352 | 2.8058 |
| | 0.2 | 0.8438 | 1.0109 | 1.7316 | 1.8588 | 1.9021 |
| | 0.5 | 0.5516 | 0.5896 | 0.7308 | 0.8458 | 0.9817 |
| | 0.8 | 0.2760 | 0.2771 | 0.2800 | 0.2896 | 0.2905 |
| 10 | 0 | 1.8480 | 3.5185 | 4.0473 | 5.9916 | 6.3512 |
| | 0.2 | 1.1563 | 1.5352 | 3.1932 | 4.1404 | 4.8849 |
| | 0.5 | 0.8621 | 0.9560 | 1.3533 | 1.6388 | 2.3101 |
| | 0.8 | 0.6470 | 0.6540 | 0.6730 | 0.6975 | 0.7545 |
| 20 | 0 | 1.8379 | 3.1941 | 4.1533 | 6.1526 | 6.4956 |
| | 0.2 | 1.1793 | 1.598 | 3.3309 | 4.4139 | 5.2045 |
| | 0.5 | 0.8877 | 0.9954 | 1.4507 | 1.7937 | 2.5902 |
| | 0.8 | 0.7279 | 0.7371 | 0.7655 | 0.7999 | 0.8775 |
| 100 | 0 | 1.8649 | 3.3264 | 4.2398 | 6.3270 | 6.7435 |
| | 0.2 | 1.1922 | 1.6442 | 3.4202 | 4.6187 | 5.3415 |
| | 0.5 | 0.8973 | 1.0154 | 1.5007 | 1.8656 | 2.6187 |
| | 0.8 | 0.7646 | 0.7753 | 0.8124 | 0.8567 | 0.9362 |

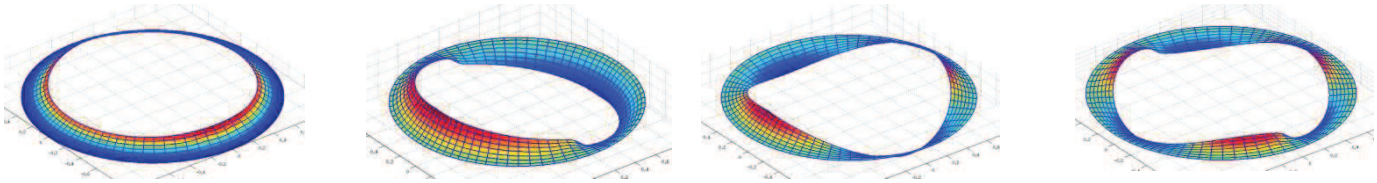

Mode 1 Mode 2 Mode 3 Mode 4

**Fig. 6** The first four mode shapes of the annular plate with r/*R*=0.8, *R/h*=10.

## 5 CONCLUSIONS

In this paper, a novel and effective formulation based on combining XIGA and HSDT has been applied to dynamic analysis of the cracked plates. The present method, utilizing NURBS basis functions, allows us to achieve easily the smoothness with arbitrary continuity order compared with the traditional FEM. Consequently, it naturally fulfills the $C^1$-continuity of HSDT model. Furthermore, the special enrichment functions are applied for describing the singularity behaviors along the crack. The obtained results are in excellent agreement with others in the literature.

## 6 REFERENCES


[1] J.N. Reddy, Analysis of functionally graded plates. International Journal for Numerical Methods in Engineering 47, 663–684, 2000.

[2] S.V. Senthil, R.C. Batra, Exact solution for thermoelastic deformations of functionally graded thick rectangular plates. AIAA Journal 40,1021–1033, 2002.

[3] H. Nguyen-Xuan, Loc V. Tran, T. Nguyen-Thoi, H.C. Vu-Do, Analysis of functionally graded plates using an edge-based smoothed finite element method. Composite Structures 93, 3019-3039, 2011.

[4] Loc V. Tran, A.J.M. Ferreira, H. Nguyen-Xuan, Isogeometric approach for analysis of functionally graded plates using higher-order shear deformation theory. Composite Part B: Engineering 51, 368-383, 2013.

[5] Loc V. Tran, Chien H. Thai, H. Nguyen-Xuan, An isogeometric finite element formulation for thermal buckling analysis of functionally graded plates, Finite Element in Analysis and Design 73, 65-76, 2013.

[6] B. Stahl, L. Keer, Vibration and stability of cracked rectangular plates. Int J Solids Struct 8, 69–91,1972.

[7] K.M. Liew, K.C. Hung, M.K. Lim, A solution method for analysis of cracked plates under vibration, Engineering Fracture Mechanics 48, 393–404, 1994.

[8] M. Bachene, R. Tiberkak, S. Rechak, Vibration analysis of cracked plates using the extended finite element method**,** Archive of Applied Mechanics 79, 249-262, 2009.

[9] G. Qian, S. Gu, J. Jiang, A finite element model of cracked plates and application to vibration problems. Comput Struct 39, 483–487, 1991.

[10] J. Dolbow, N. Moës, T. Belytschko, Modeling fracture in Mindlin–Reissner plates with the extended finite element method. Int J Solids Struct 37, 7161–7183, 2000.

[11] S.Natarajan, P.M. Baiz, S.Bordas, T.Rabczuk, P. Kerfriden, Natural frequencies of cracked FGM plates by the extended finite element method, Composite Structures 93, 3082–3092, 2011.

[12] T.J.R. Hughes, J.A. Cottrell, and Y. Bazilevs, Isogeometric analysis: CAD, finite elements, NURBS, exact geometry and mesh refinement, Computer Methods in Applied Mechanics and Engineering 194, 4135–4195, 2009.

[13] S.S. Ghorashi, N. Valizadeh, and S. Mohammadi, Extended isogeometric analysis for simulation of stationary and propagating cracks. International Journal for Numerical Methods in Engineering, 89, 1069–1101, 2012.

[14] E. De Luycker, D.J. Benson, T. Belytschko, Y. Bazilevs, and M.C. Hsu, X-FEM in isogeometric analysis for linear fracture mechanics. International Journal for Numerical Methods in Engineering 87,541–565,2011.